JOURNAL OF NATURAL PRODUCTS

ARTICLE

pubs.acs.org/jnp

Molluscicidal Metabolites from an Assemblage of Palmyra Atoll Cyanobacteria

Alban R. Pereira,[†,‡] Lena Etzbach,[†,‡,§] Niclas Engene,[†] Rolf Müller,[§] and William H. Gerwick*[,†]

[†]Center for Marine Biotechnology and Biomedicine, Scripps Institution of Oceanography, and Skaggs School of Pharmacy and Pharmaceutical Sciences, University of California, San Diego, La Jolla, California 92093, United States

[§]Helmholtz-Institute for Pharmaceutical Research Saarland, Helmholtz Center for Infectious Research, Department of Microbial Natural Products, Saarland University, Campus C2 3, 66123 Saarbrücken, Germany

Supporting Information

ABSTRACT: Molluscicides can play an important role in the control of schistosomiasis because snails of the genus *Biomphalaria* act as intermediate hosts for the parasite. Schistosomiasis is one of 13 neglected tropical diseases with high morbidity and mortality that collectively affect one billion of the world's poorest population, mainly in developing countries. Thiopalmyrone (**1**) and palmyrrolinone (**2**), metabolites isolated from extracts of a Palmyra Atoll environmental assemblage of two cyanobacteria, cf. *Oscillatoria* and *Hormoscilla* spp., represent new and potent molluscicidal chemotypes against *Biomphalaria glabrata* (LC_{50} = 8.3 and 6.0 μM, respectively). A slight enhancement in molluscicidal effect (LC_{50} = 5.0 μM) was observed when these two natural products were utilized as an equimolar binary mixture.

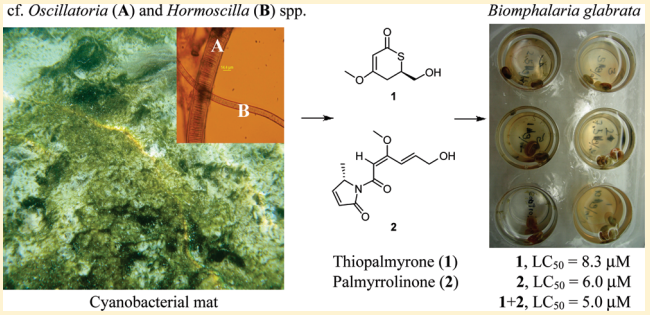

Neglected tropical diseases (NTDs) are infectious diseases that collectively affect one billion of the world's poorest population in developing countries near the equator[1] and contribute to approximately 500 000 deaths per year.[2] Commonly associated with long-term illness, impaired childhood development, disfigurement, decreased productive capabilities, and social stigma, NTDs are perpetuated by diverse factors including geographical isolation, lack of education, poor sanitation, and substandard housing conditions.[1,3] Additionally, since NTDs generally do not represent a threat to the developed world, there is little financial incentive for the pharmaceutical industry to engage in research toward developing new treatments.[4]

Although there is some variation in what constitutes a NTD, the most comprehensive account encompasses 37 conditions, with 13 core diseases causing the most significant morbidity and mortality.[1a,b,3] Three of the 13 core NTDs are protozoal (African sleeping sickness, Chagas disease, and leishmaniasis) and three are bacterial (Buruli ulcer, leprosy, and trachoma). The remaining seven diseases are caused by worms (elephantiasis, guinea worm, hookworm, river blindness, roundworm, whipworm, and schistosomiasis).[3,4b] As part as our International Cooperative Biodiversity Group (ICBG) program in Panama,[5] we have screened natural product materials for activities against malaria, leishmaniasis, Chagas disease, and schistosomiasis. In the case of schistosomiasis, molluscicides constitute an important method for the control of the disease because snails of the genus *Biomphalaria* (e.g., *B. glabrata* and *B. alexandrina*) are intermediate hosts for the parasite.[6] Thus, there is an urgent need for new water-soluble, inexpensive, and toxicity-specific molluscicidal agents that can help reduce the incidence of schistosomiasis infection and reinfection.[4a,7] Using a simple assay[8] to screen marine cyanobacterial extracts for their capacity to kill *B. glabrata*, our research group has previously discovered several molluscicidal agents, including barbamide (LC_{100} = 21.6 μM),[9] tanikolide (LC_{50} = 31.6 μM),[10] and cyanolide A (LC_{50} = 1.2 μM).[11] Here, we describe the isolation and structure elucidation of two new molluscicides, thiopalmyrone (**1**, LC_{50} = 8.3 μM) and palmyrrolinone (**2**, LC_{50} = 6.0 μM), from an assemblage of two undescribed species of cyanobacteria collected from Palmyra Atoll.

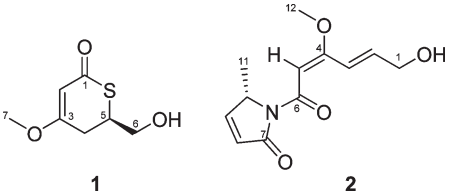

RESULTS AND DISCUSSION

A dark brown mat of cyanobacteria was collected by hand from Palmyra Atoll in the Central Pacific Ocean. The cyanobacterial collection was repeatedly extracted with CH_2Cl_2/MeOH (2:1), and a portion (4.0 g) was fractionated by silica gel vacuum liquid chromatography (VLC) to produce nine subfractions (A−I).

Received: February 2, 2011
Published: April 07, 2011

Table 1. NMR Spectroscopic Data (600 MHz, $CDCl_3$) for Thiopalmyrone (1)

carbon	δ_C, mult.[a]	δ_H, mult. (J in Hz)[b]	HMBC[c]	COSY	NOESY
1	189.0, C				
2	101.1, CH	5.46, s	3, 4a, 4b, 5	4a, 4b	7
3	174.2, C				
4a	31.3, CH_2	2.86, dd (17.1, 4.8)	2, 3, 5, 6a, 6b	2, 4b, 5	6a, 6b
4b		2.76, dd (17.1, 7.5)	2, 3, 5, 6a, 6b	2, 4a, 5	6a, 6b
5	42.8, CH	3.59, dddd (7.5, 6.6, 6.6, 4.8)	1, 3, 4a, 4b, 6a, 6b	4a, 4b, 6a, 6b	
6a	64.1, CH_2	3.81, dd (11.4, 6.6)	4a, 4b, 5	5, 6b	4a, 4b
6b		3.77, dd (11.4, 6.6)	4a, 4b, 5	5, 6a	4a, 4b
7	55.8, CH_3	3.72, s	2, 3, 4a, 4b		2

[a] Recorded at 125 MHz. [b] Recorded at 600 MHz. [c] From proton to the indicated carbon.

Fraction F (0.170 g) displayed intriguing ^{1}H NMR resonances and was thus subjected to ^{1}H NMR-guided fractionation involving gradient silica gel column chromatography, preparative TLC, and normal-phase HPLC. Two new compounds were isolated from this process, thiopalmyrone (**1**, 2.6 mg, 0.06%) and palmyrrolinone (**2**, 5.9 mg, 0.15%). In addition to these two new cyanobacterial natural products, fraction F was also found to contain the known metabolites lyngbic acid and the carotenoid zeaxanthin.[12,13]

HRESIMS of **1** yielded an $[M + H]^+$ peak at m/z 175.0421, with a complex isotopic pattern composed of m/z 175/176/177 (100:7:5 ratio), suggesting the presence of one sulfur atom. Combined with NMR data (Table 1), it was possible to derive a molecular formula of $C_7H_{10}O_3S$ (three degrees of unsaturation). Intense IR absorptions at 3420 (broad), 1732, and 1609 cm^{-1} were consistent with a hydroxy group and an α,β-unsaturated carbonyl functionality in **1**; the latter moiety was corroborated by UV absorptions at 237 and 265 nm. The ^{1}H NMR spectrum of **1** (Table 1) displayed resonances assignable to one vinyl singlet, one methoxy singlet, two diastereotopic methylene multiplets, and one methine multiplet. In agreement with these assignments, the ^{13}C NMR spectrum of **1** showed one sp^2 methine carbon and one methoxy resonance, as well as two methylene and one methine sp^3 carbons. This spectrum was completed by two deshielded quaternary carbonyl-type resonances. Extensive analysis by 2D NMR, including HSQC, HMBC, COSY, and NOESY, revealed the planar structure of thiopalmyrone (**1**) as described below.

COSY and coupling constant data revealed that the methine proton at δ 3.59 (H-5) was flanked by two diastereotopic methylene pairs, giving rise to the sole spin system present in **1**. One of these pairs was comprised of protons at δ 2.86 (H-4a) and 2.76 (H-4b), which showed an additional long-range COSY correlation with the broadened singlet proton at δ 5.46 (H-2). This vinylic methine was a component of a trisubstituted double bond with an oxygenated quaternary carbon at δ 174.2 (C-3), as revealed by HMBC correlations between the methoxy singlet at δ 3.72 (H-7) and carbon resonances at δ 101.1 (C-2), 174.2 (C-3), and 31.3 (C-4). Furthermore, an intense NOE correlation between H-2 and H-7 allowed assignment of this double bond as *E*. The second diastereotopic methylene was comprised of deshielded protons with almost isochronous chemical shift values at δ 3.81 (H-6a) and 3.77 (H-6b, δ_C 64.1), suggesting the presence of an attached oxygen atom. In agreement with the COSY-derived spin system above, HMBC correlations supported the carbon sequence C2═C3(OC7)−C4−C5−C6−O (**I** in Figure 1). An informative HMBC correlation between

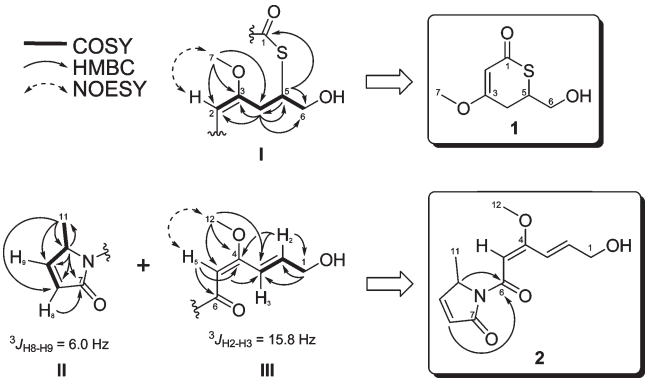

Figure 1. Partial structures for thiopalmyrone (**1**) and palmyrrolinone (**2**) derived from NMR data and their assembly by HMBC correlations.

methine H-5 (δ 3.59) and the remaining carbonyl resonance at δ 189.0 (C-1) led us to postulate a thioester linkage on the basis of the relatively shielded ^{13}C chemical shift for C-5 (δ 42.8). With all atoms in the molecular formula assigned and one unsaturation degree unaccounted for, we assembled an α,β-unsaturated thioester moiety that formed a six-membered ring, thus completing the planar structure of thiopalmyrone (**1**). This unique functional group was in agreement with the intense IR absorptions at 1732 and 1609 cm^{-1}, and the ^{1}H and ^{13}C chemical shifts were consistent with those of structurally similar synthetic model compounds.[14]

The preferred conformation between the diastereomeric methylene pair H-4a (δ 2.86)/H-4b (δ 2.76) and the adjacent methine H-5 (δ 3.59) was determined via *J*-based configuration analysis (Figure 2).[15] Homonuclear coupling constants were obtained from the ^{1}H NMR spectrum, whereas heteronuclear coupling values were obtained from HETLOC[16] and HSQMBC[17] experiments. Interestingly, intermediate values for the homonuclear $^3J_{H-5,H-4b}$ (7.5 Hz) and three out of four heteronuclear coupling constants led us to consider two major envelope-like conformers about the C-4−C-5 carbon bond where the planes of the C-1═O and C-2═C-3 double bonds are coplanar and H5/H4b exhibit both anti and gauche orientations (Figure 2A). The strong NOE correlation observed between H-2 and H-7 suggested that the methoxy group at C-7 is coplanar with the double bonds. Fortunately, the six possible rotamer pairs with the different prochiral assignments for the methylene protons were unequivocally distinguished using these various *J* values.[15] The only combination in agreement with our

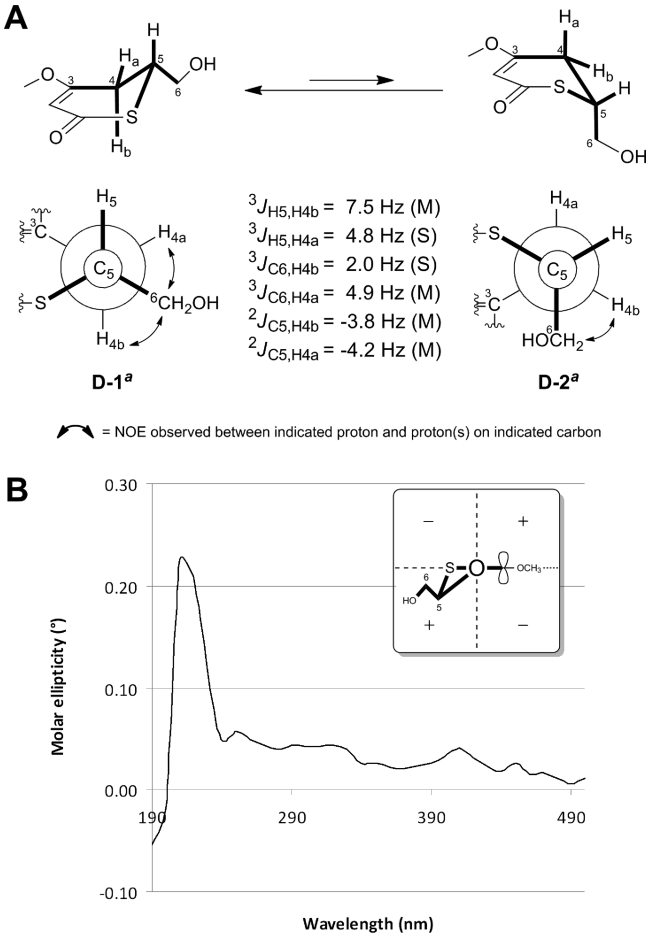

Figure 2. (A) *J*-based configuration analysis for thiopalmyrone (**1**) [S, small; M, medium; L, large; H4a is δ 2.86 (low field) and H4b is δ 2.76 (high field)]. [a]Rotamer designation according to Murata and co-workers.[15] (B) Application of Snatzke's enone sector rules for prediction of the sign of the n→π* transition (320−350 nm) in the CD spectrum of **1**.[18]

coupling constant and NOE data corresponded to the rotamer pair D-1/D-2. Because D-2 is thermodynamically disfavored due to two gauche interactions (C-6/C-3 and C-3/S), as well as repulsive electronic 1,3-diaxial interactions between the axial C-6−OH and the π bonds at C-1 and C-3 (giving rise to the carbon−oxygen and carbon−carbon double bonds, respectively), the equilibrium appears to be displaced toward the half-chair D-1 conformer. This conclusion was substantiated by medium large $^3J_{H\text{-}5,H\text{-}4b}$ and medium small $^3J_{H\text{-}5,H\text{-}4a}$ values of 7.5 and 4.8 Hz, respectively. This favored half-chair conformer with methine H-5 and methylene H-6 out of the plane was subjected to Snatzke's sector rules for planar enones.[18] This analysis predicts a positive Cotton effect for **1** exhibiting an *R* configuration at C-5 (Figure 2B), whereas the opposite could be expected for the *S* enantiomer. The CD curve for **1** showed a positive Cotton effect for the n→π* transition (320−350 nm), indicating the *R* configuration at C-5[19] and thus completing the structure of thiopalmyrone (**1**).

The second metabolite isolated, palmyrrolinone (**2**), analyzed for $C_{12}H_{15}NO_4$ (six degrees of unsaturation) by HRESIMS of an $[M + Na]^+$ peak at *m/z* 260.0895. As with **1**, intense IR bands at 3423 (broad), 3105, 1715, 1663, and 1570 cm^{-1} were consistent

Table 2. NMR Spectroscopic Data (600 MHz, $CDCl_3$) for Palmyrrolinone (2)

carbon	δ_C, mult.[a]	δ_H, mult. (*J* in Hz)[b]	HMBC[c]	COSY	NOESY
1	63.1, CH_2	4.35, dd (4.9, 1.5)	2, 3, 4, 5	2, 3	
2	137.5, CH	6.67, dt (15.8, 4.9)	1, 3, 4, 5	1, 3	
3	123.2, CH	7.53, dt (15.8, 1.5)	1, 2, 4	1, 2	
4	167.8, C				
5	94.2, CH	6.81, s	1, 2, 3, 4, 6		12
6	164.9, C				
7	170.1, C				
8	125.8, CH	6.07, dd (6.0, 1.6)	6, 7, 9, 10, 11	9, 10	
9	153.1, CH	7.21, dd (6.0, 1.9)	7, 8, 10, 11	8, 10	11
10	58.2, CH	4.88, qdd (6.6, 1.9, 1.6)	6, 7, 8, 9, 11	8, 9, 11	
11	17.9, CH_3	1.46, d (6.6)	8, 9, 10	10	9
12	55.8, CH_3	3.82, s	3, 4, 5		5

[a] Recorded at 125 MHz. [b] Recorded at 600 MHz. [c] From proton to the indicated carbon.

with the presence of a hydroxy group and an α,β-unsaturated carbonyl moiety. The latter, however, differed from that of **1** as shown by a UV absorption at 293 nm, which suggested additional conjugation. The ^{1}H NMR spectrum of **2** (Table 2) showed signals for five vinylic protons, deshielded multiplets for one sp^3 methine and one methylene, a methoxy singlet, and one final methyl doublet. Consistent with these assignments, the ^{13}C NMR spectrum of **2** possessed three oxygenated quaternary sp^2 carbons, five vinylic methine carbons, one sp^3 methine and one oxymethylene, a methoxy carbon, and a final high-field methyl carbon.

Two partial structures were assembled for **2** using the full set of 2D NMR data (**II** and **III** in Figure 1). A spin system comprising part of substructure **II** possessed a deshielded doublet methyl group (δ 1.46, H-11, d, *J* = 6.6 Hz) adjacent to three contiguous methine protons. The first of these possessed a chemical shift of δ 4.88 (H-10, qdd, *J* = 6.6, 1.6, 1.9 Hz), consistent with its attachment to a carbon bearing a heteroatom (C-10, δ 58.2). This proton was coupled vicinally and allylically to both protons of an adjacent polarized *Z* double bond constituted by protons at δ 7.21 (H-9, dd, *J* = 1.9, 6.0 Hz) and 6.07 (H-8, dd, *J* = 1.6, 6.0 Hz), thus suggesting an α,β-unsaturated amide functionality. This moiety was confirmed by HMBC correlations from protons H-8, H-9, and H-10 to a carbonyl carbon at δ 170.1, a chemical shift consistent with the amide of a pyrrolinone ring (**II**).[20]

Partial structure **III** possessed a spin system that included an oxymethylene at δ 4.35 (H-1, dd, *J* = 1.5, 4.9 Hz, δ_C 63.1) that was placed adjacent to a second polarized double bond (δ 6.67, H-2, dd, *J* = 4.9, 15.8 Hz and δ 7.53, H-3, dd, *J* = 1.5, 15.8 Hz) by COSY. These protons in turn displayed HMBC correlations with an oxygenated sp^2 quaternary carbon at δ 167.8 (C-4) and a vinylic methine carbon at δ 94.2 (C-5), thus defining a conjugated trisubstituted double bond. This second double bond was supported by HMBC correlations from the *O*-methyl singlet (H-12) as well as the vinyl proton singlet (H-5) to carbon resonances at δ 123.2 (C-3) and 167.8 (C-4), among others. The latter H-5 proton possessed an additional HMBC correlation with an amide-type carbonyl at δ 164.9 (C-6), giving rise to an $\alpha,\beta,\gamma,\delta$-unsaturated amide, thus completing partial structure **III**. The geometries of both double bonds were determined to be *E* on the basis of a $^3J_{H2,}$

$_{H3}$ value of 15.8 Hz and a strong NOE correlation between H-5 and H-12. At this point, the planar structure of **2** could be assembled by connecting partial structures **II** and **III** via HMBC correlations from H-8 and H-10 to C-6.

To determine the absolute configuration at C-10 in the pyrrolinone ring, a sample of **2** was treated with ozone followed by oxidative workup and acid hydrolysis. Chiral-phase HPLC analysis of this product revealed the presence of L-(*S*)-Ala in comparison with commercial standards, thus completing the structure of palmyrrolinone (**2**).

Pure thiopalmyrone (**1**) and palmyrrolinone (**2**) exhibited toxicity against *B. glabrata* with LC_{50} values of 8.3 and 6.0 μM, respectively. Interestingly, the molluscicidal effect was slightly enhanced [(LC_{50} = 5.0 μM) = 2.5 μM of **1** + 2.5 μM of **2**] by exposing the snails to an equimolar mixture of **1** and **2**. Thus, it is possible that thiopalmyrone (**1**) and palmyrrolinone (**2**) act synergistically by interacting with more than one cellular target. Neither metabolite was active in antifungal (*Candida albicans*) or antibacterial (MRSA) assays and were both noncytotoxic to H-460 human lung adenocarcinoma and neuro-2a murine neuroblastoma cell lines (up to a maximum test concentration of 100 μM). Thus, thiopalmyrone (**1**) and palmyrrolinone (**2**) represent two new chemotypes of relatively selective molluscicides for potential use in treating waterways infested with schistosomiasis-carrying snails of the genus *Biomphalaria*.

Biosynthetic dissection of the chemical structure of **1** suggests that it derives from a PKS pathway, whereas **2** appears to be produced by a combination of PKS and NRPS biosynthetic routes. Interestingly, thiopalmyrone (**1**) and the C1−C6 appendage of **2** share the same oxidation pattern and a similar α,β-unsaturated carbonyl moiety with *E* double-bond geometry, suggesting that they may derive from the same nascent triketide with similar elongation, reduction, and dehydration processing. The origin of the sulfur atom in **1** is uncertain, as it is difficult to envision a direct incorporation of cysteine or methionine, the usual mechanism of sulfur incorporation into cyanobacterial secondary metabolites.[21] Interestingly, thiopalmyrone (**1**) represents only the second thioester reported from a marine cyanobacterium, the other being the potent antiproliferative depsipeptide largazole.[22] Both **1** and **2** possess methoxy groups that likely derive from *S*-adenosyl methionine. However, there is a possibility that these are isolation artifacts, as one might envision them arising from the addition of MeOH to α,β-unsaturated ester or amide precursors in a Michael fashion, followed by H_2O elimination.[14b] Nevertheless, we believe these are natural features of **1** and **2**, as similar β-methoxy esters/amides are quite common structural features in other cyanobacterial metabolites (e.g., malyngamide A, barbamide, jamaicamide A).[21]

Taxonomy of the Cyanobacterial Strains. Microscopic characterization of the thiopalmyrone (**1**)- and palmyrrolinone (**2**)-producing specimen PAL 8/1/09-2 revealed that it was composed of an assemblage of two different types of filamentous cyanobacteria (Figure S17). The cyanobacterial assemblage was carefully dissected into single filaments of each type. Genomic DNA from each single filament was amplified by multiple displacement amplification (MDA) and gene sequences PCR-amplified directly from the different MDA-DNA products. Phylogenetic inference of the SSU (16S) rRNA genes of the two cyanobacteria supported their morphological differentiation and revealed that they were evolutionarily unrelated to one another (*p*-distance = 9.9% 16S rRNA gene sequence divergence, Figure 3).

Taxonomically, the two cyanobacteria both represent novel and undescribed taxa. The larger filamentous cyanobacterium PAL 8/1/09-2.1 was morphologically in agreement with the current definition of the genus *Oscillatoria* Vaucher *ex* Gomont, 1892 (for morphological description see Supporting Information).[23] However, PAL 8/1/09-2.1 (GenBank accession number JF262061) was phylogenetically relatively distant (*p*-distance = 3.9%) to the genus reference strain *O. sancta* PCC 7515.[24] Instead, PAL 8/1/09-2.1 was closely related to the ecologically distinct genus *Trichodesmium* (reference strain = IMS 101), and this paraphyly of the genus *Oscillatoria* highlights the need to taxonomically revise PAL 8/1/09-2.1 and related specimens as a new genus. Thus, in advance of such a taxonomic revision, PAL 8/1/09-2.1 is identified as cf. *Oscillatoria* sp.

The associated finely filamentous cyanobacterium PAL 8/1/09-2.2 (GenBank acc. no. JF262062) was evolutionarily most closely related to the obligate sponge-symbiont *Hormoscilla* (formerly *Oscillatoria*) *spongeliae* Anagnostidis *et* Komárek, 1988,[25] although no reference strain has been defined for this genus.[24] The phylogenetic similarity (*p*-distance = 2.8%) to *H. spongeliae* suggests that PAL 8/1/09-2.2 should also belong to the genus *Hormoscilla*. However, due to the lack of *Hormoscilla* species corresponding to PAL 8/1/09-2.2, this cyanobacterium likely represents a new species, hence, the nomenclature *Hormoscilla* sp. nov (for a morphological description see Supporting Information). Morphologically and phylogenetically similar cyanobacterial assemblages have been observed in geographically disperse tropical marine habitats, such as Curaçao, Netherlands Antilles (unpublished data). Thus, these two types of cyanobacteria appear to commonly form assemblages with one another in Nature. The fact that the strain PAL 8/1/09-2.2 represents the closest related free-living basal clade to the obligate sponge-symbiont *H. spongeliae* suggests a possible evolutionary adaptation toward symbiosis in this group of cyanobacteria.

The relative composition of the cf. *Oscillatoria* sp. and *Hormoscilla* sp. nov cyanobacteria in the consortium was approximately equivalent. Attempts to conclusively identify the actual producer of **1** and **2** in the assemblage (e.g., via MALDI imaging techniques[26]) were not successful, due in part to a lack of live cultures of either the conglomerate or the two cyanobacteria separately.

EXPERIMENTAL SECTION

General Experimental Procedures. Optical rotations were measured on a JASCO P-2000 polarimeter, whereas UV and circular dichroism data were obtained using a Beckman DU800 spectrophotometer and a JASCO J-815 CD spectrometer, respectively. IR spectra were recorded on a Nicolet 100 FT-IR spectrometer. ^{1}H, ^{13}C, and 2D NMR spectra were collected at a ^{1}H resonance frequency of either 600 MHz (Bruker Avance III DRX600 equipped with a 1.7 mm TCI cryoprobe) or 500 MHz (JEOL ECA500 and Varian VX500 equipped with a 3 mm Varian XSens cold probe). Chemical shifts were calibrated internally to the residual signal of the solvent in which the sample was dissolved ($CDCl_3$, δ_H 7.26, δ_C 77.0; CD_2Cl_2, δ_H 5.30, δ_C 53.52). High-resolution mass spectra were obtained on a ThermoFinnigan MAT900XL mass spectrometer. HPLC was carried out using a dual Waters 515 pump system equipped with a Waters 996 photodiode array detector. Vacuum and flash chromatographic separations were performed using type H (10−40 μm, Aldrich) silica and silica gel 60 (40−63 μm, EMD), respectively. Merck TLC sheets (silica gel 60 F254) were used for analytical TLC (aluminum-supported, layer thickness 200 μm) and preparative TLC (glass-supported, layer thickness 250 μm). L- and D-Alanine were acquired from Fluka and Sigma-Aldrich, respectively. All solvents were purchased as HPLC grade.

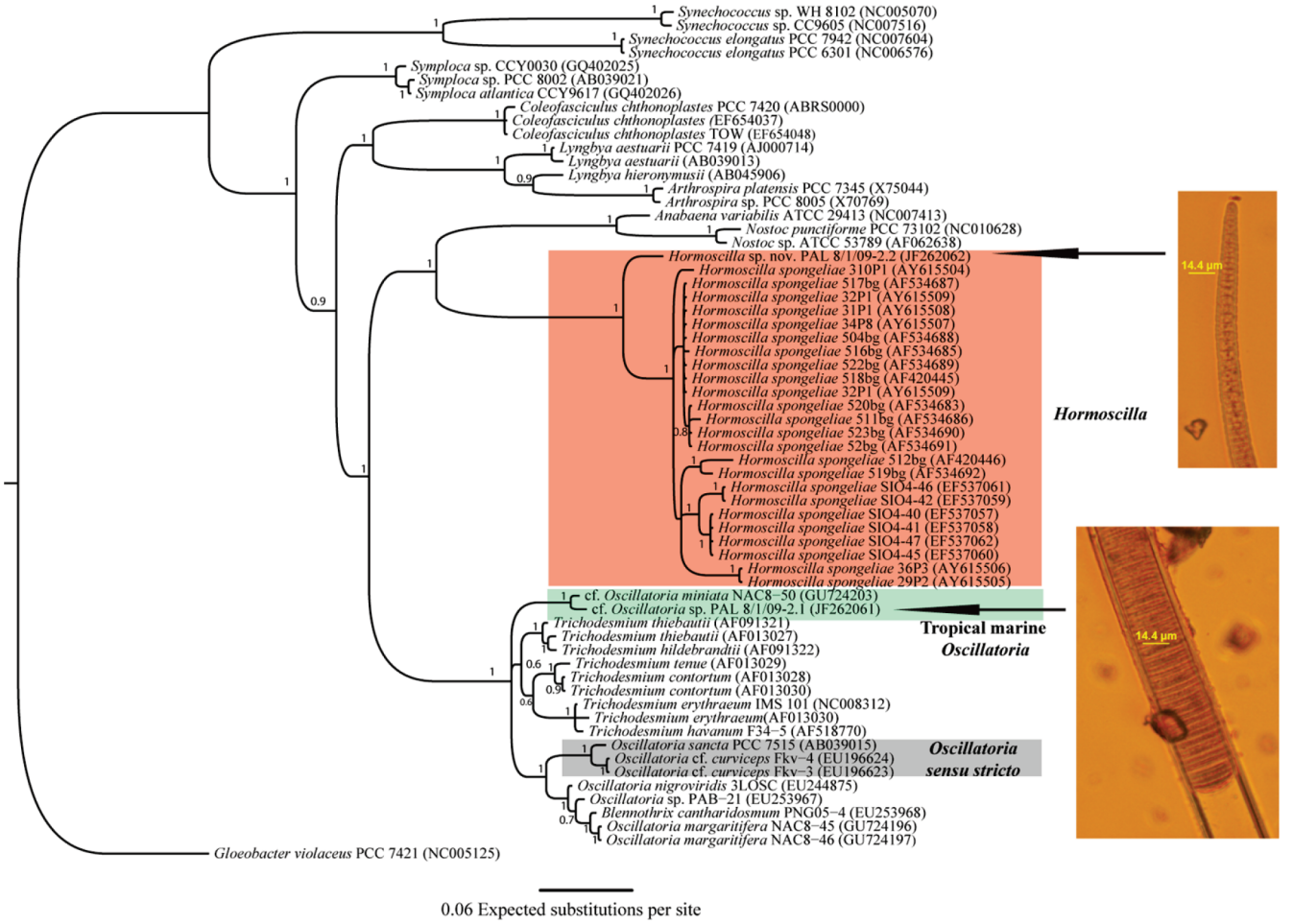

Figure 3. Evolutionary tree for the thiopalmyrone (**1**) and palmyrrolinone (**2**) producers PAL 8/1/09-2.1 and PAL 8/1/09-2.2 (highlighted with arrows). The cladogram is based on SSU (16S) rRNA gene sequences using Bayesian inference (MrBayes), and the support values are indicated as posterior probability at the nodes. The specimens are indicated as species, strain, and access number in brackets. The scale bar is indicated at 0.04 expected nucleotide substitutions per site. In the cladogram, the evolutionarily distance between the tropical marine *Oscillatoria* (green box) and the *Oscillatoria sensu stricto* (gray box), as well as the paraphyly of the genus *Oscillatoria*, indicates a need to taxonomically revise PAL 8/1/09-2.1 and related specimens as a new group. PAL 8/1/09-2.2 can be noted as a basal clade to the genus *Hormoscilla* and likely belongs to this group as a new species.

Cyanobacterial Collection and Taxonomic Identification. Samples of the cyanobacterial assemblage (voucher specimen available from W.H.G. as collection number PAL 8/1/09-2) were collected by hand at a depth of 0.5−1.5 m on flat rocks at the end of a runway at North Beach, Palmyra Atoll, in August 2009 (05°53′.831 N, 162°04′.272 W). Samples were stored in 70% EtOH at −20 °C prior to extraction. Morphological characterization was performed using an Olympus IX51 epifluorescent microscope (1000×) equipped with an Olympus U-CMAD3 camera. Morphological comparisons and putative taxonomic identification of the cyanobacterial specimen were performed in accordance with modern classification systems.[24,25]

Extraction and Isolation. Approximately 1.96 kg (dry wt) of cyanobacterial mat was extracted repeatedly with CH_2Cl_2/MeOH (2:1) to afford 4.43 g of extract. A portion of this material (4.0 g) was fractionated by silica gel vacuum liquid chromatography using a stepwise gradient of increasing polarity, starting with 10% EtOAc in hexanes and finishing with 100% MeOH, to produce nine fractions (B−I). Fraction F (eluted with 80% EtOAc in hexanes, 0.170 g) was subjected to ^{1}H NMR-guided fractionation using gradient silica gel column chromatography (20% to 60% EtOAc in hexanes), followed by preparative TLC (55% EtOAc in hexanes) and normal-phase HPLC (Phenomenex Luna 5 μm silica 100 Å, 250 × 10 mm, 50% EtOAc in hexanes at 3 mL/min, detection at 250 and 290 nm) to yield 2.6 mg of compound **1** and 5.9 mg of compound **2**. The preparative TLC step above additionally provided 19.5 mg of lyngbic acid and 3.0 mg of zeaxanthin.

*Thiopalmyrone (**1**):* colorless oil; $[\alpha]^{23}_D$ +7.6 (*c* 1.1, CH_3CN); UV (MeCN) λ_{max} 237 nm (log ε 4.06), 265 nm (log ε 3.83); CD (*c* 0.06, CH_3CN) λ_{max} ($\Delta\varepsilon$) 450 (0.03), 410 (0.04), 290 (0.04), 250 (0.06), 210 (0.22); IR (neat) 3420, 2934, 1732, 1609, 1383, 1167, 1030, 818 cm^{-1}; ^{1}H, ^{13}C, and 2D NMR data, see Table 1; HRESIMS *m*/*z* $[M + H]^+$ 175.0421 (calcd for $C_7H_{11}O_3S$, 175.0423).

*Palmyrrolinone (**2**):* colorless oil; $[\alpha]^{23}_D$ +36 (*c* 0.18, CH_3CN); UV (MeCN) λ_{max} 293 nm (log ε 4.13), 212 nm (log ε 3.97); IR (neat) 3423, 3105, 2927, 2852, 1715, 1663, 1570, 1335, 1201, 822, 756 cm^{-1}; ^{1}H, ^{13}C, and 2D NMR data, see Table 2; HRESIMS *m*/*z* $[M + Na]^+$ 260.0895 (calcd for $C_{12}H_{15}NO_4Na$, 260.0893).

Lyngbic acid: pale yellow oil; $[\alpha]^{23}_D$ −8.7 (*c* 0.04, $CHCl_3$); UV, IR, ^{1}H and ^{13}C NMR spectroscopic data were in accordance with those previously reported for the natural product;[12] HRESIMS *m*/*z* $[M + Na]^+$ 279.1934 (calcd for $C_{15}H_{28}O_3Na$, 279.1931).

Zeaxanthin: orange solid; $[\alpha]^{23}_D$ −33 (*c* 0.1, $CHCl_3$); UV, IR, ^{1}H and ^{13}C NMR spectroscopic data were in accordance with those previously reported for the natural product;[13] HREIMS *m*/*z* $[M]^+$ 568.4268 (calcd for $C_{40}H_{56}O_2$, 568.4275).

Ozonolysis, Acid Hydrolysis, and Chiral-Phase HPLC Analysis of 2. Ozone was bubbled through a sample of **2** (0.3 mg) dissolved in CH_2Cl_2 (3 mL) at 25 °C for 30 min. The solvent was evaporated, and the residue treated with 1 mL of H_2O_2/HCOOH (1:2) at 70 °C for 20 min. After removal of solvent, the ozone-treated and oxidized sample of **2** was hydrolyzed in degassed 6 M HCl (1 mL) at 110 °C for 18 h. The hydrolysate was concentrated to dryness and then dissolved in an aqueous solution of 2 mM $CuSO_4$. An aliquot of this solution was analyzed by chiral-phase HPLC [Phenomenex Chirex 3126 (D), 4.6 × 250 mm; 2 mM $CuSO_4$ in H_2O at 0.7 mL/min; detection at 254 nm] to give L-alanine (t_R 13.2 min). The retention times of authentic L-Ala and D-Ala were 12.9 and 20.6 min, respectively.

Multiple Displacement Amplification and PCR Amplification from Single Filaments. The cyanobacterial assemblage was dissected, and single filaments of the cyanobacterial components were isolated under an Olympus VMZ dissecting microscope. The single filaments were washed twice in 0.5 μL of sterile SWBG-11 medium and twice in 0.5 μL of D_2O before transfer into 0.2 mL PCR tubes. DNA was amplified from the single filaments by MDA using the REPLI-g mini kit (Qiagen), following the manufacturer's specifications. All MDA reactions were performed in 50 μL reaction volume for 16 h at 30 °C. The 16S rRNA genes were PCR-amplified from isolated DNA using the modified lineage-specific primers OT106F 5′-GGACGGGTGAGTAACGCGTGA-3′ and OT1445R 5′-AGTAATGACTTCGGGCGTG-3′. The PCR reaction volumes were 25 μL containing 0.5 μL (~50 ng) of DNA, 2.5 μL of 10× PfuUltra IV reaction buffer, 0.5 μL (25 mM) of dNTP mix, 0.5 μL of each primer (10 μM), 0.5 μL of PfuUltra IV fusion HS DNA polymerase, and 20.5 μL of D_2O. The PCR reactions were performed in an Eppendorf Mastercycler gradient as follows: initial denaturation for 2 min at 95 °C, 25 cycles of amplification, followed by 20 s at 95 °C, 20 s at 55 °C, and 1.5 min at 72 °C, and final elongation for 3 min at 72 °C. PCR products were purified using a MinElute PCR purification kit (Qiagen) before subcloning using the Zero Blunt TOPO PCR cloning kit (Invitrogen) following the manufacturer's specifications. Plasmid DNA was isolated using the QIAprep Spin miniprep kit (Qiagen) and sequenced with M13 primers. The 16S rRNA gene sequences are available in the DDBJ/EMBL/GenBank databases under acc. nos. JF262061 (PAL 8/1/09-2.1) and JF262062 (PAL 8/1/09-2.2).

Phylogenetic Inference. The 16S rRNA gene sequences of PAL-8/1/09-2.1 and PAL-8/1/09-2.2 were aligned with evolutionarily informative cyanobacteria using the L-INS-I algorithm in MAFFT 6.717[27] and refined using the SSU secondary structures model for *Escherichia coli* J01695[28] without data exclusion. The best-fitting nucleotide substitution model optimized by maximum likelihood (ML) was selected using corrected Akaike/Bayesian Information Criterion (AIC_C/BIC) in jModeltest 0.1.1.[29] The evolutionary histories of the cyanobacterial genes were inferred using maximum likelihood and Bayesian inference algorithms. The ML inference was performed using GARLI 1.0[30] for the GTR+I+G model assuming a heterogeneous substitution rate and gamma substitution of variable sites (proportion of invariable sites (pINV) = 0.422, shape parameter (α) = 0.455, number of rate categories = 4) with 1000 bootstrap replicates. Bayesian inference was conducted using MrBayes 3.1[31] with four Metropolis-coupled MCMC chains (one cold and three heated) ran for 3 000 000 generations. The first 25% were discarded as burn-in, and the following data set was being sampled with a frequency of every 100 generations. The MCMC convergence was detected by AWTY.[32]

Molluscicidal Assay. Molluscicidal activity was evaluated according to a previously outlined procedure using the test organism *Biomphalaria glabrata*.[8] In all assays, a stock solution of 20 mg/mL of pure compound in EtOH was prepared, of which 35 μL was taken and diluted to 7 mL with distilled H_2O. The snails were placed in wells of varying concentrations and observed after 24 h. If no heartbeat could be detected upon examination under a dissecting microscope (20× magnification), the snails were assessed as dead.

■ ASSOCIATED CONTENT

Supporting Information. ^{1}H NMR, ^{13}C NMR, and 2D NMR spectra in $CDCl_3$ or CD_2Cl_2 for **1** and **2**, concentration−response toxicity profiles for *B. glabrata*, morphological description of cyanobacterial specimen PAL 8/1/09-2. This material is available free of charge via the Internet at http://pubs.acs.org.

■ AUTHOR INFORMATION

Corresponding Author

*Tel: (858)-534-0578. Fax: (858)-534-0529. E-mail: wgerwick@ucsd.edu.

Author Contributions

‡A.R.P. and L.E. contributed equally to this work.

■ ACKNOWLEDGMENT

We thank A. Jones for his help in the collection of the cyanobacterial assemblage as well as The Nature Conservancy staff at Palmyra Atoll. We thank Y. Su (UCSD Mass Spectrometry) for HRMS data acquisition, T. Byrum for running mammalian cell line cytotoxicity measurements, and Prof. C. Bayne (Oregon State University) for originally supplying *B. glabrata* snails. We acknowledge the San Diego Supercomputer Center for statistical analyses using the CIPRES cluster. Support was partially provided by Fogarty International Center's International Cooperative Biodiversity Group program (NIH TW006634) and NIH CA100851. We further acknowledge the NSF CHE-0741968 for support of the JEOL and ^{13}C-sensitive Varian NMR spectrometers in the Department of Chemistry and Biochemistry, UCSD.

■ REFERENCES

(1) (a) Payne, L.; Fitchett, J. R. *Trends Parasitol.* **2010**, *26*, 421–423. (b) Hotez, P. J.; Fenwick, A.; Savioli, L.; Molyneux, D. H. *Lancet* **2009**, *373*, 1570–1575.(c) World Health Organization Control of neglected tropical diseases (NTD). http://www.who.int/neglected_diseases/en/. Accessed October 28, 2010.

(2) Molyneux, D. H.; Hotez, P. J.; Fenwick, A. *PLoS Med.* **2005**, *2*, 1064–1070.

(3) Reddy, M.; Gill, S. S.; Kalkar, S. R.; Wu, W.; Anderson, P. J.; Rochon, P. A. *JAMA* **2007**, *298*, 1911–1924.

(4) (a) Domling, A.; Khoury, K. *ChemMedChem* **2010**, *5*, 1420–1434. (b) Feasey, N.; Wansbrough-Jones, M.; Mabey, D. C. W.; Solomon, A. W. *Brit. Med. Bull.* **2010**, *93*, 179–200. (c) Trouiller, P.; Olliaro, P.; Torreele, E.; Orbinski, J.; Laing, R.; Ford, N. *Lancet* **2002**, *359*, 2188–2194.

(5) Kursar, T. A.; Caballero-George, C. C.; Capson, T. L.; Cubilla-Rios, L.; Gerwick, W. H.; Gupta, M. P.; Ibañez, A.; Linington, R. G.; McPhail, K. L.; Ortega-Barria, E.; Romero, L. I.; Solis, P. N.; Coley, P. D. *BioScience* **2006**, *56*, 1005–1012.

(6) (a) Perrett, S.; Whitfield, P. J. *Parasitol. Today* **1996**, *12*, 156–159. (b) World Health Organization. Report of the Scientific Working Group Meeting on Schistosomiasis; Geneva, Switzerland, November 14−16, 2005.

(7) (a) Bergquist, R. *Acta Trop.* **2008**, *108*, 65–68. (b) Ribeiro, K. A.; de Carvalho, C. M.; Molina, M. T.; Lima, E. P.; Lopez-Montero, E.; Reys,

J. R.; de Oliveira, M. B.; Pinto, A. V.; Santana, A. E.; Goulart, M. O. *Acta Trop.* **2009**, *111*, 44–50.
(8) Hostettmann, K.; Kizu, H.; Tomimori, T. *Planta Med.* **1982**, *44*, 34–35.
(9) Orjala, J.; Gerwick, W. H. *J. Nat. Prod.* **1996**, *59*, 427–430.
(10) Singh, I. P.; Milligan, K. E.; Gerwick, W. H. *J. Nat. Prod.* **1999**, *62*, 1333–1335.
(11) Pereira, A. R.; McCue, C. F.; Gerwick, W. H. *J. Nat. Prod.* **2010**, *73*, 217–220.
(12) (a) Cardellina, J. H.; Dalietos, D.; Marner, F. J.; Mynderse, J. S.; Moore, R. E. *Phytochemistry* **1978**, *17*, 2091–2095. (b) Kwan, J. C.; Teplitski, M.; Gunasekera, S. P.; Paul, V. J.; Luesch, H. *J. Nat. Prod.* **2010**, *73*, 463–466. (c) Chen, J.; Shi, Z. F.; Zhou, L.; Xie, A. L.; Cao, X. P. *Tetrahedron* **2010**, *66*, 3499–3507.
(13) (a) Wegerski, C. J.; France, D.; Cornell-Kennon, S.; Crews, P. *Bioorg. Med. Chem.* **2004**, *12*, 5631–5637. (b) Eisenreich, W.; Bacher, A.; Berry, A.; Bretzel, W.; Humbelin, M.; Lopez-Ulibarri, R.; Mayer, A. F.; Yeliseev, A. *J. Org. Chem.* **2002**, *67*, 871–875. (c) Englert, G.; Noack, K.; Broger, E. A.; Glinz, E.; Vecchi, M.; Zell, R. *Helv. Chim. Acta* **1991**, *74*, 969–982. (d) Moss, G. P. *Pure. Appl. Chem.* **1976**, *47*, 97–102. (e) Maoka, T.; Arai, A.; Shimizu, M.; Matsuno, T. *Comp. Biochem. Physiol.* **1986**, *83B*, 121–124. (f) Buchecker, R.; Liaaen-Jensen, S.; Borch, G.; Siegelman, H. W. *Phytochemistry* **1976**, *15*, 1015–1018.
(14) (a) Ward, D. E.; Gai, Y.; Zoghaib, W. M. *Can. J. Chem.* **1991**, *69*, 1487–1497. (b) Schweiger, K. *Monatsh. Chem.* **1982**, *113*, 1283–1297.
(15) Matsumori, N.; Kaneno, D.; Murata, M.; Nakamura, H.; Tachibana, K. *J. Org. Chem.* **1999**, *64*, 866–876.
(16) Uhrin, D.; Batta, G.; Hruby, V. J.; Barlow, P. N.; Kover, K. E. *J. Magn. Reson.* **1998**, *130*, 155–161.
(17) Williamson, R. T.; Marquez, B. L.; Gerwick, W. H.; Kover, K. E. *Magn. Reson. Chem.* **2000**, *38*, 265–273.
(18) (a) Lightner, D. A.; Gurst, J. E. *Organic Conformational Analysis and Stereochemistry from Circular Dichroism Spectroscopy*; Wiley-VCH: New York, 2000; pp 337−394. (b) Snatzke, G. *Tetrahedron* **1965**, *21*, 439–448. (c) Snatzke, G. *Tetrahedron* **1965**, *21*, 413–419. (d) Snatzke, G. *Tetrahedron* **1965**, *21*, 421–438. (e) Suga, T.; Imamura, K. *Bull. Chem. Soc. Jpn.* **1972**, *45*, 2060–2064.
(19) When the sulfur atom in thiopalmyrone (**1**) is replaced by an oxygen atom, the specific rotation of the oxygenated analogue (exhibiting also the *R* configuration) increases in magnitude but remains positive {i.e., $[\alpha]^{23}_{D}$ +187.3 (*c* 0.95, $CHCl_3$)}. See: Pospisil, J.; Marko, I. E. *Tetrahedron Lett.* **2008**, *49*, 1523–1526.
(20) (a) Meickle, T.; Matthew, S.; Ross, C.; Luesch, H.; Paul, V. *Planta Med.* **2009**, *75*, 1427–1430. (b) Edwards, D. J.; Marquez, B. L.; Nogle, L. M.; McPhail, K.; Goeger, D. E.; Roberts, M. A.; Gerwick, W. H. *Chem. Biol.* **2004**, *11*, 817–833. (c) Koehn, F. E.; Longley, R. E.; Reed, J. K. *J. Nat. Prod.* **1992**, *55*, 613–619. (d) Moore, R. E.; Entzeroth, M. *Phytochemistry* **1988**, *27*, 3101–3103.
(21) Tidgewell, K., Clark, B. T., Gerwick, W. H. In *Comprehensive Natural Products Chemistry*, 2nd ed.; Moore, B.; Crews, P., Eds.; Pergamon Press: Oxford, 2010; pp 141−188.
(22) (a) Taori, K.; Paul, V. J.; Luesch, H. *J. Am. Chem. Soc.* **2008**, *130*, 1806–1807. (b) Taori, K.; Paul, V. J.; Luesch, H. *J. Am. Chem. Soc.* **2008**, *130*, 13506–13506.
(23) Gomont, M. M. *Ann. Sci. Nat. Bot. Ser.* **1892**, *16*, 91–264.
(24) Castenholz, R. W.; Rippka, R.; Herdman, M. In *Bergey's Manual of Systematic Bacteriology*; Boone, D. R.; Castenholz, R. W., Eds.; Springer: New York, 2001; Vol. 1, pp 473−599.
(25) Komárek, J.; Anagnostidis, K. In *Süsswasserflora von Mitteleuropa*; Büdel, B.; Gärtner, G.; Krienitz, L.; Schagerl, M., Eds.; Elsevier: München, 2005; Vol 19/2, pp 441−625.
(26) Taniguchi, M.; Nunnery, J. K.; Engene, N.; Esquenazi, E.; Byrum, T.; Dorrestein, P. C.; Gerwick, W. H. *J. Nat. Prod.* **2010**, *73*, 393–398.
(27) Katoh, K.; Toh, H. *Briefings Bioinf.* **2008**, *9*, 286–298.
(28) Cannone, J. J.; Subramanin, S.; Schnare, M. N.; Collett, J. R.; D'Souza, L. M.; Du, Y.; Feng, B.; Lin, N.; Madabusi, L. V.; Muller, K. M.; Pnde, N.; Schang, Z.; Yu, N.; Gutell, R. R. *BMC Bioinf.* **2002**, *3*, 1471–2105.
(29) Posada, D. *Mol. Biol. Evol.* **2008**, *25*, 1253–1256.
(30) Zwickl, D. J. Ph.D. Thesis, University of Texas at Austin, TX, 2006.
(31) Ronquist, F.; Huelsenbeck, J. P. *Bioinformatics* **2003**, *12*, 1572–1574.
(32) Nylander, J. A. A.; Wilgenbusch, J. C.; Warren, D. L.; Swofford, D. L. *Bioinformatics* **2008**, *15*, 581–583.